Chemical Science

ROYAL SOCIETY OF CHEMISTRY

EDGE ARTICLE

View Article Online
View Journal | View Issue

Cite this: *Chem. Sci.*, 2024, **15**, 5525

All publication charges for this article have been paid for by the Royal Society of Chemistry

Received 24th December 2023
Accepted 5th March 2024

DOI: 10.1039/d3sc06925g

rsc.li/chemical-science

The superiority of Pd^{2+} in CO_2 hydrogenation to formic acid†

Yanyan Wang,[ab] Minghua Dong,[bc] Shaopeng Li,[bc] Bingfeng Chen,[b] Huizhen Liu *[bc] and Buxing Han *[bc]

The hydrogenation of CO_2 to formic acid is an essential subject since formic acid is a promising hydrogen storage material and a valuable commodity chemical. In this study, we report for the first time the hydrogenation of CO_2 to formic acid catalyzed by a Pd^{2+} catalyst, Pd–V/AC–air. The catalyst exhibited extraordinary catalytic activity toward the hydrogenation of CO_2 to formic acid. The TON and TOF are up to 4790 and 2825 h^{-1}, respectively, representing the top level among reported heterogeneous Pd catalysts. By combining a study of first-principles density functional theory with experimental results, the superiority of Pd^{2+} over Pd^0 was confirmed. Furthermore, the presence of V modified the electronic state of Pd^{2+}, thus promoting the reaction. This study reports the effect of metal valence and electronic state on the catalytic performance for the first time and provides a new prospect for the design of an efficient heterogeneous catalyst for the hydrogenation of CO_2 to formic acid.

Introduction

Nowadays, carbon dioxide chemistry has attracted extensive attention in academic and industrial communities,[1–3] since the greenhouse effect is becoming more and more serious. The catalytic hydrogenation of CO_2 to useful chemicals is one of the most effective measures to alleviate climate change and assist carbon recycling.[4–8] Among all products from CO_2 hydrogenation, formic acid (FA) is a valuable commodity chemical.[9–11] As a less-toxic, nonflammable liquid with 4.4 wt% hydrogen, it is also regarded as a promising hydrogen storage material[12,13] since the chemically stored H_2 in formic acid can be liberated in a controlled manner in the presence of appropriate catalysts, even at room temperature.[14–16] Moreover, the hydrogenation of CO_2 to FA is the first and an indispensable step in the reduction of CO_2 to other chemicals, such as methanol and hydrocarbons.[17] There is no doubt that research on CO_2 hydrogenation to FA is an essential and promising subject.[18]

The hydrogenation of CO_2 to FA involves a positive free energy ($\Delta G = 33$ kJ mol^{-1}), while the same reaction can proceed more readily in water with a negative free energy ($\Delta G = -4$ kJ mol^{-1}).[19] Similarly, the addition of a base can change the equilibrium and significantly promote the reaction. Various catalysts have been reported for the hydrogenation of CO_2 to FA.[20–28] Homogeneous metal complexes, especially Ru and Ir,[29–31] have been extensively studied and show excellent activity toward the hydrogenation of CO_2 to FA. However, the activity of heterogeneous catalysts lags a lot in spite of it showing obvious advantages in product separation and catalyst recycling.[18] Therefore, there is great demand for heterogeneous catalysts with excellent activity, and it is certainly desirable to find special properties of heterogenous catalysts that affect the performance and study of the structure–activity relationship.

For the hydrogenation of CO_2 to FA, the most widely researched heterogeneous catalysts are supported Pd catalysts.[32–36] As we all know, the catalytic performance of supported metal catalysts is largely determined by the electronic properties of the catalyst surface.[37–39] The modification of the metal center[40] and support[41] can change the electronic properties of the catalyst surface. The introduction of a second metal could greatly improve the catalytic performance because of the electronic effect between two metals.[42,43] Electron-rich Pd centers are created with the aid of neighboring Ag atoms in a PdAg catalyst, which boost the electronegativity of dissociated hydride species and thus facilitate the reaction.[44] A Pd@Ag alloy exhibited a turnover number of 2496 based on the quantity of all employed Pd atoms. A zeolite-encaged metallic PdMn catalyst exhibited extraordinary catalytic activity and durability in CO_2 hydrogenation into formate due to ultrasmall metal clusters and electron-rich Pd surface resulting from the synergistic effect between Pd and Mn components, and the formate generation rate during CO_2 hydrogenation reached 2151 $mol_{formate}$ mol_{Pd}^{-1} h^{-1} at 353 K.[45] It has been demonstrated that the introduction

[a]National Narcotics Laboratory Beijing Regional Center, Beijing 100164, P. R. China
[b]Beijing National Laboratory for Molecular Sciences, Key Laboratory of Colloid and Interface and Thermodynamics, CAS Research/Education Center for Excellence in Molecular Sciences, Institute of Chemistry, Chinese Academy of Sciences, Beijing 100190, China. E-mail: liuhz@iccas.ac.cn; hanbx@iccas.ac.cn
[c]School of Chemical Science, University of Chinese Academy of Sciences, Beijing 100049, China

† Electronic supplementary information (ESI) available. See DOI: https://doi.org/10.1039/d3sc06925g

of an amine group to the support could also promote the reaction rate toward the hydrogenation of CO_2 to FA.[46–48] The introduction of amine could increase the adsorption capacity of the catalyst to CO_2. More importantly, it can change the electronic structure of the Pd center and put Pd into a positive state. Although it has been recognized that Pd in a positive state is beneficial to the reaction, reported catalysts are often pre-reduced to zero-valent palladium prior to use. It is unknown for the catalytic performance of Pd in a positive state, especially for divalent palladium.

In this study, we have synthesized Pd–V/AC–air through calcination of the Pd precursor supported on activated carbon (AC) in air, in which Pd is in divalent state. It exhibited extraordinary catalytic activity toward the hydrogenation of CO_2 to FA. The TON and TOF can be up to 4790 and 2825 h^{-1}, respectively, both representing the top level among all the heterogeneous Pd catalysts. First-principles density functional theory (DFT) calculations show that the energy barrier for the reaction over PdO is lower than that over Pd^0, which demonstrates the superiority of Pd^{2+} for the hydrogenation of CO_2 to FA.

Results and discussions

Synthesis and characterization of the catalyst

The Pd–V/AC–air catalyst was prepared by an impregnation method. It was obtained by impregnation of palladium(II) acetylacetonate and vanadium(IV)oxy acetylacetonate on AC and later calcined in air at 300 °C. The preparation of the Pd–V/AC–H_2 catalyst is similar except that the precursor was reduced in 10%H_2/Ar at 300 °C. The details and preparation of other catalysts are shown in the ESI.†

Fig. 1a shows the transmission electron microscopy (TEM) image of prepared Pd–V/AC–air, where the mean particle size is about 10 nm, similar to that of prepared Pd/AC–air, Pd/AC–H_2 and Pd–V/AC–H_2 (Fig. S1†). The crystalline structures of prepared Pd heterogeneous catalysts were characterized by X-ray diffraction (XRD), and the results are displayed in Fig. 1b. The PdO diffraction peak at 33.7 is clearly visible for the Pd/AC–air catalyst (PDF# 46-1107). The disappearance of the PdO diffraction peak in the Pd–V/AC–air catalyst may result from the partial occupation of oxygen by the introduced V. Pd–V/AC–H_2 and Pd/AC–H_2 catalysts show a Pd diffraction peak at 40.1 (PDF# 46-1043). X-ray photoelectron spectroscopy (XPS) measurements were used to study the surface electronic state of the Pd–V/AC–air and the Pd–V/AC–H_2 catalysts. For Pd–V/AC–air, peaks at 337.55 eV and 342.74 eV are attributed to Pd^{2+} $3d_{5/2}$ and Pd^{2+} $3d_{3/2}$, respectively (Fig. 1c).[49] For Pd–V/AC–H_2, peaks at 335.40 eV and 340.75 eV are attributed to Pd^0 $3d_{5/2}$ and Pd^0 $3d_{3/2}$, respectively (Fig. 1d). These illustrate that Pd species in Pd–V/AC–air exist in the state of Pd^{2+}, whereas most palladium species have been reduced to Pd^0 in the Pd–V/AC–H_2 catalyst.[49] The XPS of Pd/AC–air and Pd/AC–H_2 were also analysed, and the results are displayed in Fig. S2.† Similar results were obtained, where the Pd species in Pd/AC–air exist in the state of Pd^{2+}, whereas they are Pd^0 in the Pd/AC–H_2 catalyst. The ICP-AES suggests that the contents of palladium and vanadium in Pd–V/AC–air are 0.61% and 0.49%, respectively.

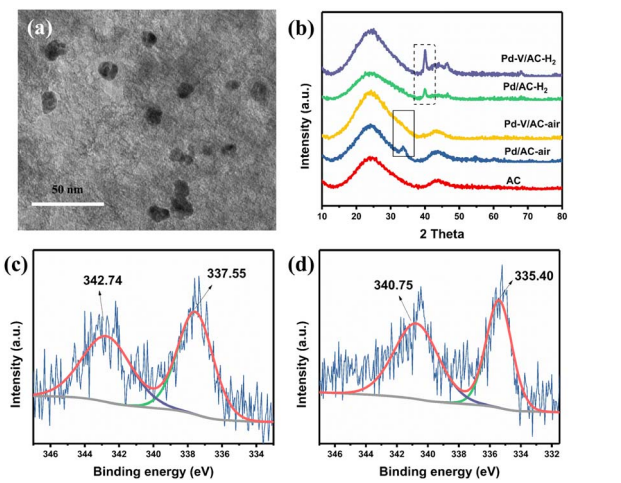

Fig. 1 (a) TEM image of the Pd–V/AC–air catalyst. (b) XRD patterns of various Pd heterogeneous catalysts. (c) XPS spectra of Pd for the Pd–V/AC–air catalyst. (d) XPS spectra of Pd for the Pd–V/AC–H_2 catalyst.

The superiority of Pd^{2+}

The hydrogenation of CO_2 to FA was carried out in a basic aqueous solution containing 1.0 M Na_2CO_3 under a total pressure of 6.0 MPa ($H_2/CO_2 = 1:1$) at 120 °C over 12 h (Table 1). Pd–V/AC–air exhibited excellent catalytic performance. The TON and TOF of the FA can be up to 4790 and 2825 h^{-1}, respectively (Table 1, entry 2). Both these values are superior to those of the reported heterogeneous Pd catalysts for the hydrogenation of CO_2 to FA (Table S1†). The catalytic performance of Pd/AC–air was also tested, and it showed much lower catalytic activity than Pd–V/AC–air, where the TON of FA is 2968 and the TOF is only 983 h^{-1} (Table 1, entry 1). This shows that the introduction of V could improve the catalytic activity and enhance the reaction rate a lot in spite of the low activity of V/AC itself (Table 1, entry 6). Compared with the Pd/AC–H_2 catalyst, Pd/AC–air showed higher activity (Table 1, entries 1 and 3). Furthermore, the activity of Pd–V/AC–air is more than 20 times that of the Pd–V/AC–H_2 catalyst (Table 1, entries 2 and 4). These results demonstrate the superiority of Pd^{2+} compared to the Pd^0 catalyst for the hydrogenation of CO_2 to FA. Besides, we calcined Pd–V/AC–H_2 and obtained the catalyst Pd–V/AC–H_2–air, and

Table 1 Hydrogenation of CO_2 to FA over various catalysts[a]

Entry	Catalyst	Pd valence	TON	TOF[b]	Sel. (%)
1	Pd/AC–air	+2	2968	983	>99
2	Pd–V/AC–air	+2	4790	2825	>99
3	Pd/AC–H_2	0	143	0	>99
4	Pd–V/AC–H_2	0	143	164	≥99
5	Pd–V/AC–H_2–air	—	2047	—	>99
6	V/AC	—	0	—	—

[a] Reaction conditions: catalyst (5 mg), 1.0 M Na_2CO_3 (2 mL), P_{H_2} (3 MPa), P_{CO_2} (3 MPa), T (120 °C), t (12 h). [b] TOF was calculated at 0.5 h.

Pd–V/AC–H_2–air exhibited much better catalytic performance than Pd–V/AC–H_2 and the TON of HCOOH increased to 2047 (Table 1, entry 5), which identifies the active site for this catalytic system as Pd^{2+}. For all the heterogeneous Pd catalysts tested in this research, the selectivity for FA was more than 99%, and no other product was detected in the reaction system.

Considering the good performance of Pd–V/AC–air, other reaction conditions were optimized. Na_2CO_3 was proved to be the best additive base among those bases we checked (Table S2†). The effect of total pressure and pressure ratio of H_2/CO_2 was also studied. When H_2 pressure is greater than 3 MPa, CO_2 pressure has little effect on the TON and TOF values. 3 MPa H_2 and 1 MPa CO_2 are enough to obtain a satisfactory TON for FA (Table S3†).

To investigate electronic and structural information of the Pd species in heterogeneous Pd catalysts, X-ray absorption near-edge structure spectroscopy (XANES) and extended X-ray absorption fine structure spectroscopy (EXAFS) of Pd/AC–air, Pd–V/AC–air and Pd–V/AC–H_2 were measured, and EXAFS fitting data are listed in Table S6.† As shown in Fig. 2a, the K-edge XANES spectra of Pd/AC–air and Pd–V/AC–air were found to resemble that of PdO. In the Pd K-edge Fourier-transformed EXAFS spectra, a peak at about 1.6 Å attributed to the Pd–O bond was observed for the Pd/AC–air and Pd–V/AC–air catalysts (Fig. 2c). Nevertheless, the K-edge XANES spectrum of the Pd–V/AC–H_2 catalyst is similar to that of Pd foil (Fig. 2a), and the peak at about 2.5 Å, attributed to the Pd–Pd bond in the Pd K-edge Fourier-transformed EXAFS spectrum, was obvious (Fig. 2c). These results illustrate that the Pd species exist as Pd^{2+} in the Pd/AC–air and Pd–V/AC–air catalysts and as Pd^0 in the Pd–V/AC–H_2 catalyst, consistent with XPS results. It is noteworthy that there is a slight difference in the Pd white-line intensity between Pd/AC–air and Pd–V/AC–air (Fig. 2b). The Pd white-line intensity for Pd–V/AC–air is slightly lower than that for Pd/AC–air, which indicates a higher electron density of the Pd species in the Pd–V/AC–air catalyst. The EXAFS fitting data of the Pd–V/AC–air catalyst demonstrates that there exists a Pd–O–V structure, which may result in the slightly higher electron density of the Pd species (Table S6 and Fig. S3†). The introduction of the second metal V modified the electronic environment of the Pd^{2+} species and thus improved the catalytic performance toward the hydrogenation of CO_2 to FA since V/AC has no catalytic activity (Table 1, entry 6).

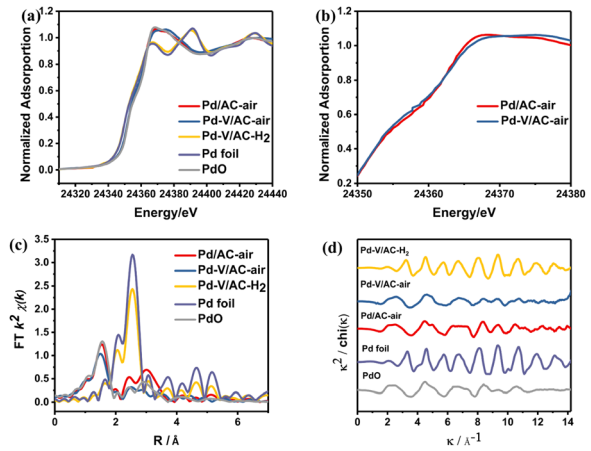

Fig. 2 (a) Normalized Pd K-edge XANES spectra of Pd/AC–air, Pd–V/AC–air, Pd–V/AC–H_2, Pd foil and PdO. (b) Extended spectra of normalized Pd K-edge XANES spectra of Pd/AC–air and Pd–V/AC–air. (c) Fourier transform of k^2-weighted EXAFS spectra and (d) EXAFS oscillations of Pd/AC–air, Pd–V/AC–air, Pd–V/AC–H_2, Pd foil and PdO at the Pd K-edge.

DFT study

To better understand the superiority of the Pd^{2+} catalyst over the Pd^0 catalyst, DFT calculations were performed. The most stable Pd (111) slab was chosen as the structural model for the Pd^0 catalyst, and the Pd^{2+} catalyst was represented by the PdO (101) slab since the PdO (101) facet possesses the lowest surface energy among the four possible PdO facets (Fig. S4†).

Next, we probed the reaction energetics of the hydrogenation of CO_2 to FA, and the resulting potential energy diagram and schematic diagrams of transition states are shown in Fig. 3. The energies of studied intermediates and transition states are tabulated in Table S7.† In the case of the PdO (101) slab, the heterolytic dissociation of H_2 occurs *via* TS1 with a barrier of 0.32 eV. Following this step, the adsorbed CO_2 is attacked by the hydride through TS2 with a barrier of 0.43 eV. Next, the adsorbed proton is transferred to the oxygen of the adsorbed HCOO* and forms the adsorbed HCOOH* through TS3. Finally, HCOOH* desorbs from the PdO surface. In the case of the Pd (111) slab, the reaction pathway is similar except that the dissociation of H_2 is neglected since the dissociation of H_2 on the Pd surface is so easy that hydrogen atoms are assumed to adsorb on the surface directly.[50] The results show that the rate-determining step of the hydrogenation of CO_2 to FA is the attack of the hydride on the adsorbed CO_2. The barrier of the rate-determining step on the PdO (101) slab (0.43 eV) is much lower than that on the Pd (111) slab (1.48 eV), and it is noticeable that the potential energy diagram of PdO (101) (Fig. 3, blue lines) is flatter than that of Pd (111) (Fig. 3, red lines). In this way, the hydrogenation of CO_2 to FA is proved to be more efficient on PdO, and it further illustrates the superiority of Pd^{2+} for the hydrogenation of CO_2 to FA.

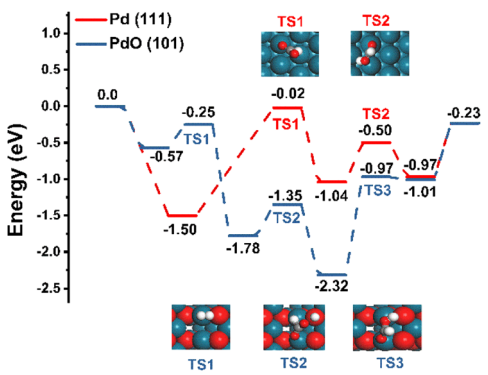

Fig. 3 Potential energy profiles for the hydrogenation of CO_2 to FA on the PdO (101) slab and Pd (111) slab. Structures of transition states are shown in insets. Blue: Pd; red: O; grey: C; white: H.

Conclusions

In summary, we prepared a Pd^{2+} catalyst, Pd–V/AC–air, and it exhibited excellent catalytic performance toward the hydrogenation of CO_2 to FA. The TON and TOF can be up to 4790 and 2825 h^{-1}, respectively, both of which are higher than those of the reported heterogeneous Pd catalysts. Furthermore, Pd–V/AC–air showed much higher activity than Pd–V/AC–H_2, indicating the superiority of Pd^{2+} over Pd^0. DFT calculations displayed that the rate-determining step of hydrogenation of CO_2 to FA was the attack of the hydride on the adsorbed CO_2, and the barrier of this step over PdO is much lower than that over Pd. In addition, the EXAFS illustrates that the introduction of V modifies the electronic structure of the Pd species and thus improves the catalytic performance. To the best of our knowledge, the important role of Pd^{2+} in the hydrogenation of CO_2 to FA was demonstrated for the first time. This study provides guidelines for the design of a heterogeneous catalyst and a direction for further research into the hydrogenation of CO_2 to FA *via* heterogeneous catalyst.

Data availability

Essential data are fully provided in the main text and ESI.† Further data in this study are available from corresponding authors upon a reasonable request.

Author contributions

Yanyan Wang conceived and designed the project, which was supervised by Huizhen Liu and Buxing Han. Yanyan Wang conducted the majority of the experimental work. Minghua Dong designed and carried out all DFT calculations. The EXAFS measurement and data analysis were done by Minghua Dong, Shaopeng Li and Bingfeng Chen. Yanyan Wang and Minghua Dong prepared the manuscript. All authors discussed, commented on, and revised the manuscript.

Conflicts of interest

There are no conflicts to declare.

Acknowledgements

This work was supported by the National Key Research and Development Program of China (2023YFA1506804) and the National Natural Science Foundation of China (22293012, 22179132, 22121002, and 22302209).

Notes and references

1 R.-P. Ye, J. Ding, W. Gong, M. D. Argyle, Q. Zhong, Y. Wang, C. K. Russell, Z. Xu, A. G. Russell, Q. Li, M. Fan and Y.-G. Yao, CO_2 hydrogenation to high-value products *via* heterogeneous catalysis, *Nat. Commun.*, 2019, **10**, 5698–5712.

2 X. Jiang, X. Nie, X. Guo, C. Song and J. G. Chen, Recent Advances in Carbon Dioxide Hydrogenation to Methanol via Heterogeneous Catalysis, *Chem. Rev.*, 2020, **15**, 7984–8034.

3 W. Zhou, K. Cheng, J. Kang, C. Zhou, V. Subramanian, Q. Zhang and Y. Wang, New horizon in C1 chemistry: breaking the selectivity limitation in transformation of syngas and hydrogenation of CO_2 into hydrocarbon chemicals and fuels, *Chem. Soc. Rev.*, 2019, **48**, 3193–3228.

4 X. Ye, C. Yang, X. Pan, J. Ma, Y. Zhang, Y. Ren, X. Liu, L. Li and Y. Huang, Highly Selective Hydrogenation of CO_2 to Ethanol via Designed Bifunctional Ir_1-In_2O_3 Single-Atom Catalyst, *J. Am. Chem. Soc.*, 2020, **142**, 19001–19005.

5 L. Ding, T. Shi, J. Gu, Y. Cui, Z. Zhang, C. Yang, T. Chen, M. Lin, P. Wang, N. Xue, L. Peng, X. Guo, Y. Zhu, Z. Chen and W. Ding, CO_2 Hydrogenation to Ethanol over Cu@Na-Beta, *Chem*, 2020, **6**, 2673–2689.

6 C. Wang, E. Guan, L. Wang, X. Chu, Z. Wu, J. Zhang, Z. Yang, Y. Jiang, L. Zhang, X. Meng, B. C. Gates and F. S. Xiao, Product Selectivity Controlled by Nanoporous Environments in Zeolite Crystals Enveloping Rhodium Nanoparticle Catalysts for CO_2 Hydrogenation, *J. Am. Chem. Soc.*, 2019, **141**, 8482–8488.

7 L. Wang, E. Guan, Y. Wang, L. Wang, Z. Gong, Y. Cui, X. Meng, B. C. Gates and F. S. Xiao, Silica accelerates the selective hydrogenation of CO_2 to methanol on cobalt catalysts, *Nat. Commun.*, 2020, **11**, 1033–1041.

8 K. W. Ting, T. Toyao, S. M. A. H. Siddiki and K.-I. Shimizu, Low-Temperature Hydrogenation of CO_2 to Methanol over Heterogeneous TiO_2-Supported Re Catalysts, *ACS Catal.*, 2019, **9**, 3685–3693.

9 G. H. Gunasekar, K. Park, K.-D. Jung and S. Yoon, Recent developments in the catalytic hydrogenation of CO_2 to formic acid/formate using heterogeneous catalysts, *Inorg. Chem. Front.*, 2016, **3**, 882–895.

10 Y. Wang, Y. Liu, L. Tan, X. Lin, Y. Fang, X. F. Lu, Y. Hou, G. Zhang and S. Wang, Confining ultrafine Pt nanoparticles on In2O3 nanotubes for enhanced selective methanol production by CO_2 hydrogenation, *J. Mater. Chem. A*, 2023, **11**, 26804–26811.

11 X. Lin, S. Wang, W. Tu, Z. Hu, Z. Ding, Y. Hou, R. Xu and W. Dai, MOF-derived hierarchical hollow spheres composed of carbon-confined Ni nanoparticles for efficient CO_2 methanation, *Catal. Sci. Technol.*, 2019, **9**, 731–738.

12 K. Sordakis, C. Tang, L. K. Vogt, H. Junge, P. J. Dyson, M. Beller and G. Laurenczy, Homogeneous Catalysis for Sustainable Hydrogen Storage in Formic Acid and Alcohols, *Chem. Rev.*, 2018, **118**, 372–433.

13 Z. Li and Q. Xu, Metal-Nanoparticle-Catalyzed Hydrogen Generation from Formic Acid, *Acc. Chem. Res.*, 2017, **50**, 1449–1458.

14 D. Mellmann, P. Sponholz, H. Junge and M. Beller, Formic acid as a hydrogen storage material - development of homogeneous catalysts for selective hydrogen release, *Chem. Soc. Rev.*, 2016, **45**, 3954–3988.

15 J.-M. Yan, S.-J. Li, S.-S. Yi, B.-R. Wulan, W.-T. Zheng and Q. Jiang, Anchoring and Upgrading Ultrafine NiPd on Room-Temperature-Synthesized Bifunctional NH_2-N-rGO toward Low-Cost and Highly Efficient Catalysts for Selective Formic Acid Dehydrogenation, *Adv. Mater.*, 2018, **30**, 1703038.

16 W. Hong, M. Kitta, N. Tsumori, Y. Himeda, T. Autrey and Q. Xu, Immobilization of highly active bimetallic PdAu nanoparticles onto nanocarbons for dehydrogenation of formic acid, *J. Mater. Chem. A*, 2019, **7**, 18835–18839.

17 M. D. Porosoff, B. Yan and J. G. Chen, Catalytic reduction of CO_2 by H_2 for synthesis of CO, methanol and hydrocarbons: challenges and opportunities, *Energy Environ. Sci.*, 2016, **9**, 62–73.

18 Q. Liu, X. Yang, L. Li, S. Miao, Y. Li, Y. Li, X. Wang, Y. Huang and T. Zhang, Direct catalytic hydrogenation of CO_2 to formate over a Schiff-base-mediated gold nanocatalyst, *Nat. Commun.*, 2017, **8**, 1407.

19 S. Moret, P. J. Dyson and G. Laurenczy, Direct synthesis of formic acid from carbon dioxide by hydrogenation in acidic media, *Nat. Commun.*, 2014, **5**, 4017–4023.

20 T. Zhao, X. Hu, Y. Wu and Z. Zhang, Hydrogenation of CO_2 to Formate with H_2: Transition Metal Free Catalyst Based on a Lewis Pair, *Angew. Chem., Int. Ed.*, 2019, **58**, 722–726.

21 H.-K. Lo, I. Thiel and C. Coperet, Efficient CO_2 Hydrogenation to Formate with Immobilized Ir-Catalysts Based on Mesoporous Silica Beads, *Chem.-Eur. J.*, 2019, **25**, 9443–9446.

22 Z. Li, T. M. Rayder, L. Luo, J. A. Byers and C.-K. Tsung, Aperture-Opening Encapsulation of a Transition Metal Catalyst in a Metal-Organic Framework for CO_2 Hydrogenation, *J. Am. Chem. Soc.*, 2018, **140**, 8082–8085.

23 J. A. Laureanti, G. W. Buchko, S. Katipamula, Q. Su, J. C. Linehan, O. A. Zadvornyy, J. W. Peters and M. O'Hagan, Protein Scaffold Activates Catalytic CO_2 Hydrogenation by a Rhodium Bis(diphosphine) Complex, *ACS Catal.*, 2019, **9**, 620–625.

24 G. Liu, P. Poths, X. Zhang, Z. Zhu, M. Marshall, M. Blankenhorn, A. N. Alexandrova and K. H. Bowen, CO_2 Hydrogenation to Formate and Formic Acid by Bimetallic Palladium-Copper Hydride Clusters, *J. Am. Chem. Soc.*, 2020, **142**, 7930–7936.

25 S. Coufourier, Q. G. Gaillard, J.-F. Lohier, A. Poater, S. Gaillard and J.-L. Renaud, Hydrogenation of CO_2, Hydrogenocarbonate, and Carbonate to Formate in Water using Phosphine Free Bifunctional Iron Complexes, *ACS Catal.*, 2020, **10**, 2108–2116.

26 K. Niu, L. Chen, J. Rosen and J. Björk, CO_2 Hydrogenation with High Selectivity by Single Bi Atoms on MXenes Enabled by a Concerted Mechanism, *ACS Catal.*, 2024, **14**, 1824–1833.

27 G. Ji, C. Li, B. Fan, G. Wang, Z. Sun, M. Jiang, L. Ma, L. Yan and Y. Ding, Single Ru-P Site Catalyst Coupling N Sites in a Flexible Polymeric Framework for Efficient CO_2 Hydrogenation to Formate, *ACS Catal.*, 2024, **14**, 1595–1607.

28 V. Mehar, W. Liao, M. Mahapatra, R. Shi, H. Lim, I. Barba-Nieto, A. Hunt, I. Waluyo, P. Liu and J. A. Rodriguez, Morphology Dependent Reactivity of CsOx Nanostructures on Au(111): Binding and Hydrogenation of CO_2 to HCOOH, *ACS Nano*, 2023, **17**, 22990–22998.

29 D. P. Estes, M. Leutzsch, L. Schubert, A. Bordet and W. Leitner, Effect of Ligand Electronics on the Reversible Catalytic Hydrogenation of CO_2 to Formic Acid Using Ruthenium Polyhydride Complexes: A Thermodynamic and Kinetic Study, *ACS Catal.*, 2020, **10**, 2990–2998.

30 R. Kanega, N. Onishi, D. J. Szalda, M. Z. Ertem, J. T. Muckerman, E. Fujita and Y. Himeda, CO_2 Hydrogenation Catalysts with Deprotonated Picolinamide Ligands, *ACS Catal.*, 2017, **7**, 6426–6429.

31 A. Weilhard, M. I. Qadir, V. Sans and J. Dupont, Selective CO_2 Hydrogenation to Formic Acid with Multifunctional Ionic Liquids, *ACS Catal.*, 2018, **8**, 1628–1634.

32 Z. Zhang, L. Zhang, M. J. Hülsey and N. Yan, Zirconia phase effect in Pd/ZrO_2 catalyzed CO_2 hydrogenation into formate, *Mol. Catal.*, 2019, **475**, 110461.

33 C. Mondelli, B. Puertolas, M. Ackermann, Z. Chen and J. Perez-Ramirez, Enhanced Base-Free Formic Acid Production from CO_2 on $Pd/g\text{-}C_3N_4$ by Tuning of the Carrier Defects, *ChemSusChem*, 2018, **11**, 2859–2869.

34 Y. Wu, Y. Zhao, H. Wang, B. Yu, X. Yu, H. Zhang and Z. Liu, 110th Anniversary: Ionic Liquid Promoted CO_2 Hydrogenation to Free Formic Acid over Pd/C, *Ind. Eng. Chem. Res.*, 2019, **58**, 6333–6339.

35 J. F. Qu, S. Q. Li, Z. Y. Deng, J. D. Hu, X. G. Yang, Y. H. Cai, F. Du, B. L. Zhong, C. M. Li and Q. M. Sun, Charge polarization-modulated $Pd\text{-}Ni(OH)_2$ hybrids in mesoporous silica SBA-15 for efficient low-temperature CO_2 hydrogenation to formate, *Chem. Eng. J.*, 2023, **467**, 143405.

36 X. Xiao, J. J. Gao, S. B. Xi, S. Lim, A. K. W. Peng, A. Borgna, W. Chu and Y. Liu, Experimental and in situ DRIFTs studies on confined metallic copper stabilized Pd species for enhanced CO_2 reduction to formate, *Appl. Catal., B*, 2022, **309**, 121239.

37 W. Zhang, L. Wang, H. Liu, Y. Hao, H. Li, M. U. Khan and J. Zeng, Integration of Quantum Confinement and Alloy Effect to Modulate Electronic Properties of RhW Nanocrystals for Improved Catalytic Performance toward CO_2 Hydrogenation, *Nano Lett.*, 2017, **17**, 788–793.

38 S. Bai, Q. Shao, Y. Feng, L. Bu and X. Huang, Highly Efficient Carbon Dioxide Hydrogenation to Methanol Catalyzed by Zigzag Platinum-Cobalt Nanowires, *Small*, 2017, 131604311.

39 K. Mori, T. Taga and H. Yamashita, Isolated Single-Atomic Ru Catalyst Bound on a Layered Double Hydroxide for Hydrogenation of CO_2 to Formic Acid, *ACS Catal.*, 2017, **7**, 3147–3151.

40 K. Mori, H. Hata and H. Yamashita, Interplay of Pd ensemble sites induced by GaOx modification in boosting CO_2 hydrogenation to formic acid, *Appl. Catal., B*, 2023, **320**, 122022.

41 J. Zhang, W. Liao, H. Zheng, Y. Zhang, L. Xia, B.-T. Teng, J.-Q. Lu, W. Huang and Z. Zhang, Morphology-engineered highly active and stable Pd/TiO_2 catalysts for CO_2 hydrogenation into formate, *J. Catal.*, 2022, **405**, 152–163.

42 C. Wu, M. W. Luo, Y. J. Zhao, S. P. Wang, A. Zavabeti, P. Y. Xiao and G. K. Li, CO_2 hydrogenation using MOFs encapsulated PdAg nano-catalysts for formate production, *Chem. Eng. J.*, 2023, **475**, 146411.

43 S. Li, M. Dong, M. Peng, Q. Mei, Y. Wang, J. Yang, Y. Yang, B. Chen, S. Liu, D. Xiao, H. Liu, D. Ma and B. Han, Crystal-phase engineering of PdCu nanoalloys facilitates selective

hydrodeoxygenation at room temperature, *Innovation*, 2022, **3**, 100189.

44 K. Mori, T. Sano, H. Kobayashi and H. Yamashita, Surface Engineering of a Supported PdAg Catalyst for Hydrogenation of CO_2 to Formic Acid: Elucidating the Active Pd Atoms in Alloy Nanoparticles, *J. Am. Chem. Soc.*, 2018, **140**, 8902–8909.

45 Q. Sun, B. W. J. Chen, N. Wang, Q. He, A. Chang, C. M. Yang, H. Asakura, T. Tanaka, M. J. Hulsey, C. H. Wang, J. Yu and N. Yan, Zeolite-Encaged Pd-Mn Nanocatalysts for CO_2 Hydrogenation and Formic Acid Dehydrogenation, *Angew. Chem., Int. Ed.*, 2020, **59**, 20183–20191.

46 S. Masuda, K. Mori, Y. Kuwahara and H. Yamashita, PdAg nanoparticles supported on resorcinol-formaldehyde polymers containing amine groups: the promotional effect of phenylamine moieties on CO_2 transformation to formic acid, *J. Mater. Chem. A*, 2019, **7**, 16356–16363.

47 S. Masuda, K. Mori, Y. Futamura and H. Yamashita, PdAg Nanoparticles Supported on Functionalized Mesoporous Carbon: Promotional Effect of Surface Amine Groups in Reversible Hydrogen Delivery/Storage Mediated by Formic Acid/CO_2, *ACS Catal.*, 2018, **8**, 2277–2285.

48 K. Mori, S. Masuda, H. Tanaka, K. Yoshizawa, M. Che and H. Yamashita, Phenylamine-functionalized mesoporous silica supported PdAg nanoparticles: a dual heterogeneous catalyst for formic acid/CO_2-mediated chemical hydrogen delivery/storage, *Chem. Commun.*, 2017, **53**, 4677–4680.

49 Y. Wang, B. Chen, S. Liu, X. Shen, S. Li, Y. Yang, H. Liu and B. Han, Methanol Promoted Palladium-Catalyzed Amine Formylation with CO_2 and H_2 by the Formation of $HCOOCH_3$, *ChemCatChem*, 2018, **10**, 5124–5127.

50 W. Dong, G. Kresse and J. Hafner, Dissociative adsorption of H_2 on the Pd(111) surface, *J. Mol. Catal. A: Chem.*, 1997, **119**, 69–76.